Superconductivity in $SrPd_2Ge_2$

H. Fujii[1,*] and A. Sato[2]
[1]*Superconducting Materials Center, National Institute for Materials Science, 1-2-1 Sengen, Tsukuba, Ibaraki 305-0047, Japan*
[2]*Materials Analysis Station, National Institute for Materials Science, 1-1 Namiki, Tsukuba, Ibaraki 305-0044, Japan*
(Received 3 April 2009; revised manuscript received 24 May 2009; published 19 June 2009)

Ternary germanide $SrPd_2Ge_2$ has been prepared by arc melting. The crystal structure of this germanide was determined by single-crystal x-ray diffraction. This is isostructural with the recently discovered superconductors $(Ba,Sr)_{1-x}(K,Cs)_xFe_2As_2$ with $ThCr_2Si_2$-type structure with space group $I4/mmm$. The lattice parameters of $SrPd_2Ge_2$ are $a=0.440\,88(2)$ and $c=1.012\,70(8)$ nm. dc magnetization and electrical resistivity measurements indicated that the $SrPd_2Ge_2$ is a type II superconductor with a critical temperature (T_c) of 3.04 K.

DOI: 10.1103/PhysRevB.79.224522 PACS number(s): 74.70.Dd, 61.05.cp, 61.66.Fn, 74.25.Op

I. INTRODUCTION

Among ternary intermetallic compounds, $ThCr_2Si_2$-type intermetallics have been extensively studied, especially for the interest of the superconducting and magnetic properties. The structure of $ThCr_2Si_2$ is the ordered ternary derivative of the binary $BaAl_4$-type structure.[1] Although numerous $ThCr_2Si_2$-type intermetallics have been reported so far, superconductivity is observed only for some compounds. The critical temperature (T_c) of those compounds is generally very low, as reported for $LaPd_2Ge_2$ and $LaIr_2Ge_2$ with T_c's of 1.12 (Ref. 2) and 1.5 K,[3] respectively.

Many works were carried out for the discovery of new intermetallic superconductors with higher T_c's. Some intermetallic superconductors with relatively high T_c's, such as MgB_2 with AlB_2-type structure,[4] were reported so far. Concerning the $ThCr_2Si_2$-type structure, quaternary intermetallics RET_2B_2C with $ThCr_2Si_2$-derivative structure were discovered.[5–8] Among these borocarbides, YPd_2B_2C shows the highest T_c of 23 K. Furthermore, recently new $ThCr_2Si_2$-type superconductors $(Ba,Sr)_{1-x}(K,Cs)_xFe_2As_2$ were discovered with T_c's up to 38 K.[9,10] Thus, this structure is one of the keys to search new intermetallic superconductors with higher T_c's. In this paper we report one of the $ThCr_2Si_2$-type superconductors, $SrPd_2Ge_2$, with a T_c of 3.04 K.

II. EXPERIMENTAL

Starting materials were Sr (sheet, 99% in purity), Pd (sheet, 99.95%), and Ge (grain, 99.99%). They were arc melted with a stoichiometric ratio of $SrPd_2Ge_2$ under Ar gas atmosphere on a water-cooler copper hearth. The melting was repeated several times with the button turned over between each melt. First Pd and Ge were arc melted and then the melted buttons were melted together with Sr in order to minimize the loss of Sr. The weight loss after the melting was within a few percent. The obtained buttons wrapped in a Ti foil were annealed in an evacuated silica tube at 1173 K for one week and quenched into a cold water bath.

Phase identification was carried out for crushed samples by an x-ray diffraction (XRD) method with an x-ray diffractometer JEOL JDX-3500 with monochromatized Cu $K\alpha$ radiation. Single crystals for structural analyses picked up from the crushed samples were glued on the top of a glass fiber and mounted on the goniometer head. X-ray single-crystal diffraction data were collected at room temperature 293(2) K using a Bruker SMART APEX charge-coupled device (CCD) area-detector diffractometer with graphite monochromatized Mo $K\alpha$ radiation ($\lambda=0.071\,073$ nm). The absorption correction and structural refinement were carried out using the programs SADABS and SHELXL97.[11,12] Microstructural observation was carried out using a scanning electron microscope (SEM) JEOL JSM-6301F with an energy dispersive x-ray (EDX) spectrometer.

dc magnetization measurements were performed for polycrystalline bulk samples with a superconducting quantum interference device (SQUID) magnetometer Quantum Design MPMS XL. Field-dependent and temperature-dependent magnetization $[M(H)$ and $M(T)]$ curves were recorded at temperatures above 1.8 K in fields up to 2 kOe. The volume fraction of superconducting phase was estimated from the magnitude of zero-field cooling (ZFC) magnetization in a field of 10 Oe in the $M(T)$ measurements. The T_c was defined as the onset temperature where a diamagnetic signal was observed. Electrical resistivity (ρ) measurements were carried out for polycrystalline samples in the temperature range from 1.8 to 300 K in magnetic fields up to 1.2 kOe by a standard dc four-probe method. Each measurement was carried out for a few samples to check reproducibility.

III. RESULTS AND DISCUSSION

A. Structural analyses

Figure 1 shows the XRD pattern of crushed powder sample of $SrPd_2Ge_2$. Most of the diffraction peaks in the XRD pattern are indexed on the basis of a tetragonal unit cell with lattice parameters of $a=0.441$ and $c=1.013$ nm. The reflection condition is $h+k+l=2n$. This indicates that the lattice is body centered with one of suggested space groups $I\bar{4}m2$, $I\bar{4}2m$, $I4mm$, $I422$, and $I4/mmm$. SEM-EDX analyses were performed on the polished cross section of the button of $SrPd_2Ge_2$. The composition of the main phase in these samples is Sr:Pd:Ge=1:2:2, indicating that the phase with the tetragonal cell is indeed $SrPd_2Ge_2$.

Shiny crystals picked up from the crushed samples were used for structural refinement. Preliminary investigations indicated that these crystals have nearly the same lattice parameters as the crushed samples mentioned above.

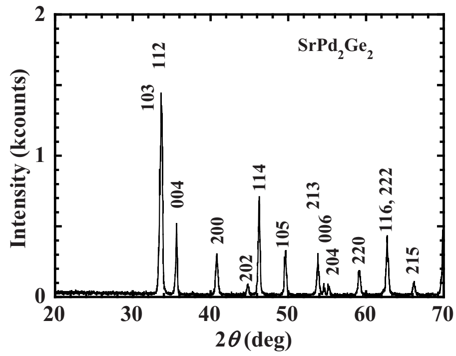

FIG. 1. XRD pattern of crushed polycrystalline sample of $SrPd_2Ge_2$. Most of the XRD peaks are indexed on the basis of a tetragonal unit cell with the lattice parameters of $a=0.411$ and $c=1.013$ nm.

The lattice parameters of $SrPd_2Ge_2$ are almost equal to other $ThCr_2Si_2$-type intermetallics with space group $I4/mmm$. For example, the parameters of $SrRh_2Ge_2$ with this structure are $a=0.4183$ and $c=1.0718$ nm.[13] Therefore, the structural refinements were first carried out on the basis of the model of the $ThCr_2Si_2$-type structure. Table I lists the atomic coordinates and equivalent thermal parameters. The crystal data and the results of structural refinements are listed in Table II. The small R factors indicate that the structure of $SrPd_2Ge_2$ is $ThCr_2Si_2$ type. Compared with the lattice parameters of $ThCr_2Si_2$-type $SrNi_2Ge_2$ with the lattice parameters of $a=0.4188$ and $c=1.0254$ nm,[14] replacement of Ni with a larger atom Pd causes quite a large elongation of the a axis parameters, whereas the c axis parameters are almost the same. The same trend is observed for LaM_2Ge_2 (M=Ni and Pd). The lattice parameters of $LaNi_2Ge_2$ are $a=0.4187$ and $c=0.9918$ nm,[14] whereas $LaPd_2Ge_2$ shows $a=0.43669$ and $c=1.0027$ nm.[15]

B. Superconducting properties

Figure 2 shows temperature-dependent dc magnetization measured in both ZFC and field cooling (FC) modes for $SrPd_2Ge_2$. The diamagnetic signals are observed at 3.04 K for both modes with a 10%–90% transition width (ΔT_c) of about 0.1 K. The as-melted $SrPd_2Ge_2$ samples show a slightly higher T_c of 3.10 K with a ΔT_c of 0.15 K. The detail of the region in the vicinity of T_c is shown in the inset. The magnitude of the magnetic shielding signal after being corrected for demagnetization effects is approximately equal to 100% of that estimated for perfect diamagnetism, while the magnitude of flux expulsion (Meissner effect) is 7% of that estimated for perfect diamagnetism. These indicate that the superconductivity is a bulk effect. Taking account of the existence of hysteresis observed between the signals in ZFC and FC modes, we conclude that the $SrPd_2Ge_2$ is a type II superconductor.

Figure 3 shows the $M(H)$ curves measured at various temperatures for $SrPd_2Ge_2$. The details of the same curves in the background region are shown in the inset. These curves are characteristic for type II superconductors. Figure 4 shows the $M(T)$ curves measured for $SrPd_2Ge_2$ at various magnetic fields. The details of the same curves in the vicinity of T_c are also shown in the inset.

Figure 5 shows the electrical resistivity ρ as a function of temperature in magnetic fields. The resistivity decreases with decreasing temperature, showing metalliclike conductivity. From 300 to 30 K, the temperature-dependent resistivity curve shows a small negative curvature. Such a curvature is also observed for $U_3Ni_4Si_4$-type $La_3M'_4X_4$ (M'=Ni and Pd, X=Si and Ge) superconductors consisting of the combination of structural units of AlB_2-type $LaM'X$ and $ThCr_2Si_2$-type LaM'_2X_2 layers.[16,17] The onset temperature of the transition in 0 Oe is 3.09 K and zero resistance is observed at 3.03 K. The

TABLE II. Crystal data and results of the structural refinements for $SrPd_2Ge_2$.

	$SrPd_2Ge_2$
Space group	$I4/mmm$ (No.139)
Lattice parameters	
a (nm)	0.44088(2)
c (nm)	1.01270(8)
Cell volume (nm^3)	0.19684(2)
f.u./cell	$Z=2$
Calculated density (g cm^{-3})	7.518
Crystal size (μm^3)	$60\times60\times80$
Absorption coefficient (mm^{-1})	37.27
R_{int}	0.0212
$2\theta_{max}$	80.7
Number of measured reflections	2057
Number of unique reflections	215
Number of reflections with $I>2\sigma(I)$	200
hkl range	$-7\leq h\leq7$, $-7\leq k\leq7$, $-18\leq l\leq14$
Number of refined parameters	9
Final residual $R[F^2>2\sigma(F^2)]$	0.0188
Weighted $R(F^2)$	0.0450
Goodness of fit on F^2	1.157
Highest/lowest electron density (eÅ^{-3})	0.84/−1.10

TABLE I. Atomic coordinates and equivalent thermal parameters for $SrPd_2Ge_2$.

Atom	Wyckoff position	x	y	z	$U_{eq}\times10^4$ (nm^2)
Sr	2a	0	0	0	1.46(1)
Pd	4d	0	1/2	1/4	1.88(1)
Ge	4e	0	0	0.37034(5)	1.68(1)

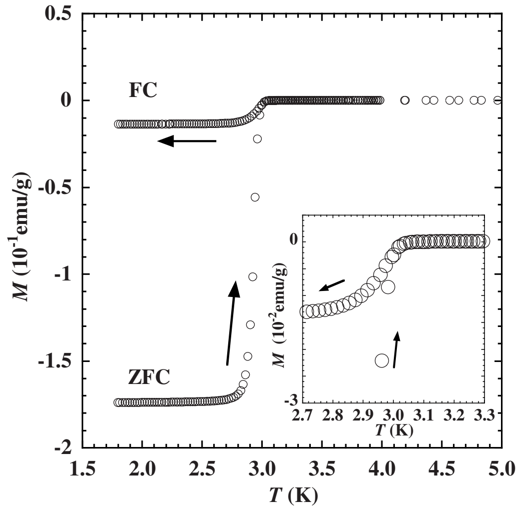

FIG. 2. Temperature-dependent dc magnetization curves for polycrystalline sample of $SrPd_2Ge_2$. The data were recorded in ZFC and FC modes. The applied field was 10 Oe. The details of the same curves in the vicinity of T_c are shown in the inset.

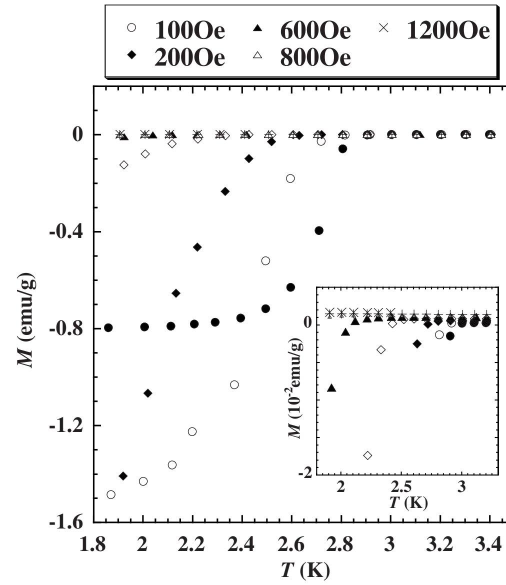

FIG. 4. Temperature dependence of magnetization $M(T)$ curves at various magnetic fields for polycrystalline sample of $SrPd_2Ge_2$. The details of the same curves in the vicinity of T_c are shown in the inset.

detail of the region in the vicinity of T_c is shown in the inset. The room-temperature resistivity, $\rho(300\ \mathrm{K})$, is approximately 30 $\mu\Omega$ cm and the residual resistivity, $\rho(\mathrm{res})$, just above T_c is 2.5 $\mu\Omega$ cm. Therefore, the residual resistivity ratio is $\rho(300\ \mathrm{K})/\rho(\mathrm{res})=12$, indicating that the sample has a good quality. With increasing applied magnetic fields, the T_c decreases and zero resistance is no longer observed in fields above 600 Oe.

The apparent lower critical field (H_{c1}^*) was determined by low-field magnetization measurements with the SQUID magnetometer. H_{c1}^* at various temperatures was taken as the point of deviation of $M(H)$ from the linear M-H behavior observed at low fields. The true lower critical field (H_{c1}) was obtained from the H_{c1}^* by applying the correction for the demagnetization factor. The H_{c1} as a function of temperature is shown in Fig. 6. Fitting the formula $H_{c1}=H_{c1}(0)[1-(T/T_c)^2]$, $H_{c1}(0)=180$ Oe and $T_c=3.0$ K are obtained. The $H_{c1}(0)$ is much lower than that of the $ThCr_2Si_2$-derivative borocarbide superconductors (around 800 Oe),[18] whereas the recently discovered same $ThCr_2Si_2$-type $BaNi_2P_2$ superconductor shows comparable $H_{c1}(0)$. It is reported that $BaNi_2P_2$ has a range of T_c. Polycrystalline $BaNi_2P_2$ with a T_c of 3 K shows $H_{c1}=150$ Oe at 1.9 K,[19] while single crystalline $BaNi_2P_2$ with a T_c of 2.51 K shows H_{c1} of about 80 and 50 Oe at 2 K for $H\|$ and $\perp c$, respectively.[20]

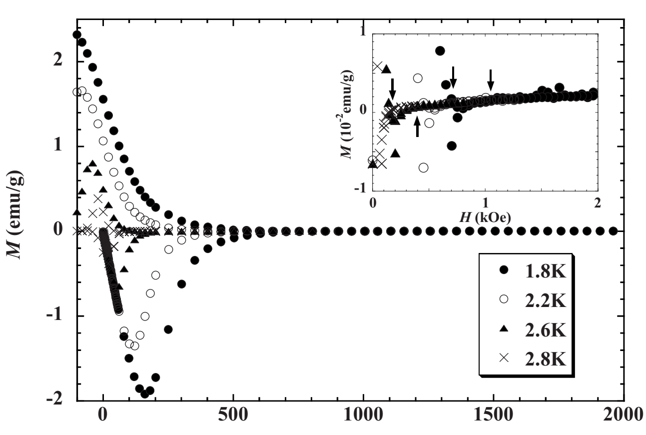

FIG. 3. Field dependence of magnetization $M(H)$ curves at various temperatures for polycrystalline sample of $SrPd_2Ge_2$. The details of the same curves in the background region are shown in the inset. The points where the $M(H)$ curves reach the background are indicated by arrows for each temperature.

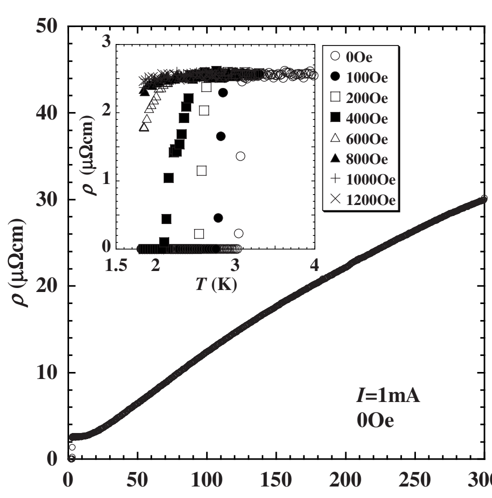

FIG. 5. Temperature-dependent electrical resistivity ρ for polycrystalline sample of $SrPd_2Ge_2$ in $H=0$ Oe. The inset shows the detail of the region in the vicinity of T_c in various magnetic fields. The applied current I was 1 mA.

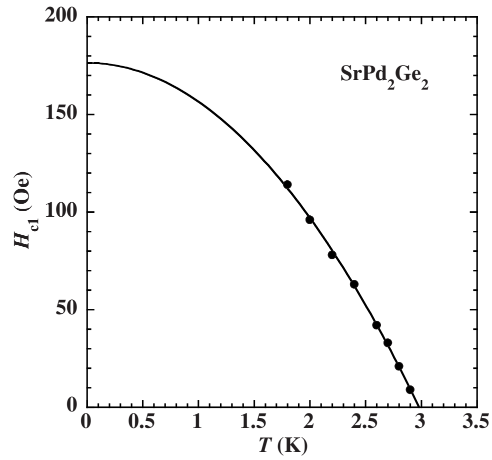

FIG. 6. Lower critical field H_{c1} as a function of temperature for polycrystalline sample of $SrPd_2Ge_2$. The H_{c1} data are fitted with the formula $H_{c1}=H_{c1}(0)[1-(T/T_c)^2]$.

The upper critical field (H_{c2}) was estimated from both $M(H)$ and $M(T)$ curves. For the $M(H)$ curves, the H_{c2} was determined from the point where the $M(H)$ curves reach the background. For the $M(T)$ curves, the H_{c2} was estimated, taking account of the onset point of superconducting transition of the $M(T)$ curves. The H_{c2} estimated from these curves as a function of temperature is shown in Fig. 7. The gradient $-dH_{c2}/dT$ is estimated to be 0.84 and 0.83 kOe/K for $H_{c2}^{M\text{-}H}(T)$ and $H_{c2}^{M\text{-}T}(T)$ curves, respectively. These values are much lower than those of the same $ThCr_2Si_2$-type $(Ba,K)Fe_2As_2$ and $ThCr_2Si_2$-derivative borocarbides. The $-dH_{c2}/dT$ of the $(Ba,K)Fe_2As_2$ single crystal is 29 and 54 kOe/K for $H\|c$ and $H\perp c$, respectively.[21] The borocarbides

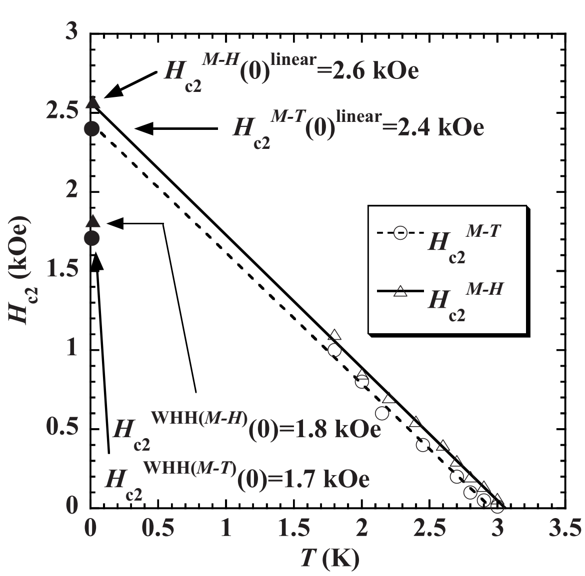

FIG. 7. Upper critical field H_{c2} obtained from $M(T)$ and $M(H)$ curves as a function of temperature for polycrystalline sample of $SrPd_2Ge_2$. The $H_{c2}^{M\text{-}T}(0)$ and $H_{c2}^{M\text{-}H}(0)$ denoted by a solid circle and a solid triangle are estimated by linear extrapolation of the $H_{c2}(T)$ curves obtained from the $M(T)$ and $M(H)$ curves, respectively. The $H_{c2}(0)^{\mathrm{WHH}}$ estimated by the WHH formula for these curves is also denoted by the same symbols as indicated by arrows.

TABLE III. Measured and derived superconducting parameters for $SrPd_2Ge_2$.

T_c (K)	3.04
$H_c(0)$ (Oe)	770
$H_{c1}(0)$ (Oe)	180
$H_{c2}(0)$ (kOe)	1.8
$-dH_{c2}/dT$ (kOe/K)	0.84
$\lambda(0)$ (nm)	71
$\xi(0)$ (nm)	43
$\kappa(0)$	1.6

show the $-dH_{c2}/dT$ value of 8 kOe/K.[18] On the other hand, the same $ThCr_2Si_2$-type $BaNi_2P_2$ single crystal with a T_c of 2.51 K shows the comparable $-dH_{c2}/dT$ values of about 0.4 and 1 kOe/K for $H\|$ and $\perp c$, respectively.[20]

Linear extrapolation of the $H_{c2}(T)$ curves obtained from the $M(H)$ and $M(T)$ curves gives $H_{c2}^{M\text{-}H}(0)=2.6$ kOe and $H_{c2}^{M\text{-}T}(0)=2.4$ kOe, respectively. On the other hand, assuming the Werthamer-Hefland-Hohemberg (WHH) formula $H_{c2}^{\mathrm{WHH}}(0)=-0.69T_c(dH_{c2}/dT)_{Tc}$,[22] $H_{c2}^{\mathrm{WHH}}(0)$ values of 1.8 and 1.7 kOe are obtained from $H_{c2}^{M\text{-}H}(0)$ and $H_{c2}^{M\text{-}T}(0)$ curves, respectively. $H_{c2}^{\rho\text{-}T}(T)$ which is defined as the field where the 1% decrease in ρ at the superconducting transition of the $\rho(T)$ curves is observed in Fig. 5 gives $-dH_{c2}/dT$ $=1.0$ kOe/K and $H_{c2}^{\mathrm{WHH}}(0)=2.1$ kOe. In the following calculations, we have used intermediate $H_{c2}^{\mathrm{WHH}(M\text{-}H)}(0)$ for $H_{c2}(0)$ among these three values.

With the formula $H_{c2}(0)=\Phi_0/2\pi\xi(0)^2$ (Φ_0 is the flux quantum), the Ginzburg-Landau (GL) coherence length $\xi(0)$ is estimated to be 43 nm. From $H_{c2}(0)$ and $\xi(0)$ the penetration depth, $\lambda(0)$, is calculated to be 71 nm with the formula $H_{c1}(0)=[\Phi_0/4\pi\lambda(0)^2]\ln[\lambda(0)/\xi(0)]$. The GL parameter, $\kappa(0)[=\lambda(0)/\xi(0)]$, is 1.6. This value of the GL parameter is quite small. It is noted that $LaPd_2Ge_2$, obtained by the replacement of Sr with La in $SrPd_2Ge_2$, is a type I superconductor with a T_c of 1.12 K.[2] On the other hand, thermodynamic critical field $[H_c(0)]$ is estimated to be 770 Oe, with the formula of $H_c(0)=H_{c2}(0)/\sqrt{2}\kappa(0)$. Table III lists these measured and calculated superconducting properties for $SrPd_2Ge_2$.

IV. CONCLUSIONS

We have prepared ternary germanide $SrPd_2Ge_2$ by arc melting. This is isostructural with the recently discovered $ThCr_2Si_2$-type superconductors $(Ba,Sr)_{1-x}(K,Cs)_xFe_2As_2$ with space group $I4/mmm$. The lattice parameters of $SrPd_2Ge_2$ are $a=0.440\,88(2)$ and $c=1.012\,70(8)$ nm. dc magnetization and electrical resistivity measurements indicated that the $SrPd_2Ge_2$ is a type II superconductor with a T_c of 3.04 K.

ACKNOWLEDGMENTS

The authors cordially thank H. Takeya and K. Hirata for their help in the electrical resistivity measurements.

*Corresponding author.

[1] Z. Ban and M. Sikirica, Acta Crystallogr. **18**, 594 (1965).
[2] G. W. Hull, J. H. Wernick, T. H. Geballe, J. V. Waszczak, and J. E. Bernardini, Phys. Rev. B **24**, 6715 (1981).
[3] M. Francois, G. Venturini, J. F. Maréché, B. Malaman, and B. Roques, J. Less-Common Met. **113**, 231 (1985).
[4] J. Nagamatsu, N. Nakagawa, T. Muranaka, Y. Zenitani, and J. Akimitsu, Nature (London) **410**, 63 (2001).
[5] R. J. Cava, H. Takagi, B. Batlogg, H. W. Zandbergen, J. J. Krajewski, W. F. Peck, Jr., R. B. van Dover, R. J. Felder, T. Siegrist, K. Mizuhashi, J. O. Lee, H. Eisaki, S. A. Carter, and S. Uchida, Nature (London) **367**, 146 (1994).
[6] R. J. Cava, H. Takagi, H. W. Zandbergen, J. J. Krajewski, W. F. Peck, Jr., T. Siegrist, B. Batlogg, R. B. van Dover, R. J. Felder, K. Mizuhashi, J. O. Lee, H. Eisaki, and S. Uchida, Nature (London) **367**, 252 (1994).
[7] R. J. Cava, B. Batlogg, T. Siegrist, J. J. Krajewski, W. F. Peck, Jr., S. Carter, R. J. Felder, H. Takagi, and R. B. van Dover, Phys. Rev. B **49**, 12384 (1994).
[8] H. Fujii, S. Ikeda, T. Kimura, S. Arisawa, K. Hirata, H. Kumakura, K. Kadowaki, and K. Togano, Jpn. J. Appl. Phys., Part 1 **33**, L590 (1994).
[9] M. Rotter, M. Tegel, and D. Johrendt, Phys. Rev. Lett. **101**, 107006 (2008).
[10] K. Sasmal, B. Lv, B. Lorenz, A. M. Guloy, F. Chen, Y.-Y. Xue, and C.-W. Chu, Phys. Rev. Lett. **101**, 107007 (2008).
[11] Bruker, SMART, SAINT, and SADABS, Bruker AXS, Inc., Madison, Wisconsin, USA, 2001.
[12] G. M. Sheldrick, Acta Crystallogr., Sect. A: Found. Crystallogr. **64**, 112 (2008).
[13] J. González, R. Kessens, and H. U. Schuster, Z. Anorg. Allg. Chem. **619**, 13 (1993).
[14] W. Rieger and E. Parthé, Monatsch. Chem. **100**, 444 (1969).
[15] G. Venturini and B. Malaman, J. Alloys Compd. **235**, 201 (1996).
[16] H. Fujii, T. Mochiku, H. Takeya, and A. Sato, Phys. Rev. B **72**, 214520 (2005).
[17] H. Fujii, J. Phys.: Condens. Matter **18**, 8037 (2006).
[18] H. Takagi, R. J. Cava, H. Eisaki, J. O. Lee, K. Mizuhashi, B. Batlogg, S. Uchida, J. J. Krajewski, and W. F. Peck, Jr., Physica C **228**, 389 (1994).
[19] T. Mine, H. Yanagi, T. Kamiya, Y. Kamihara, M. Hirano, and H. Hosono, Solid State Commun. **147**, 111 (2008).
[20] Y. Tomioka, T. Ito, H. Kito, A. Iyo, H. Eisaki, S. Ishida, M. Nakajima, and S. Uchida, J. Phys. Soc. Jpn. **77** Suppl. C, 136 (2008).
[21] H. Q. Yuan, J. Singleton, F. F. Balakirev, S. A. Baily, G. F. Chen, J. L. Luo, and N. L. Wang, Nature (London) **457**, 565 (2009).
[22] N. R. Werthamer, E. Helfand, and P. C. Hohemberg, Phys. Rev. **147**, 295 (1966).